Characteristics of Coseismic Thrust-Related Folding from Paleoseismic Investigation Responsible for the 1999 Chi-Chi Earthquake of Central Taiwan

Wen-Shan Chen[1], Nobuhisa Matsuta[2] and Chih-Cheng Yang[3]

[1]Department of Geosciences, National Taiwan University, Choushan Road, Taipei, Taiwan
[2]Research Center for Seismology, Volcanology and Disaster Mitigation Graduate School of Environmental Studies, Nagoya University D2-2(510), Furo-cho, Chikusa-ku, Nagoya, Zip,
[3]Taiwan Petroleum Exploration Division, Chinese Petroleum Corporation, Miaoli, Taiwan,
[1,3]Republic of China
[2]Japan

1. Introduction

The Western Foothills are a west-verging fold-thrust belt related to the recent arc-continent collision of the Asian continental plate with the Philippine Sea plate (Suppe, 1981). The frontal orogenic belt of Western Foothills consists of well constructed imbricated thrust faults, which have recently been locked and rooted into an aseismic decollement (Chen *et al.*, 2001c; Yue *et al.*, 2005). Over the past tens years, several great intraplate thrust earthquakes (Mw >7.0) located at the orogenic belt occurred in the world (e.g., the 2008 Wenchuan earthquake and the 1999 Chi-Chi earthquake). On September 21, 1999, central Taiwan was hit by an earthquake of magnitude Mw 7.6. Several buildings and infrastructure were severely damaged, and about 2450 people were killed. The Chi-Chi earthquake was caused by a thrust fault located at the boundary between the Western Foothills and the Taichung piggyback basin; the fault produced a spectacular surficial rupture of 100 km in length (Fig. 1; Central Geological Survey, 1999; Chen *et al.*, 2001c). Based on seismic reflection profiles and focal mechanisms of the mainshock, it was inferred that the earthquake occurred on a shallow-dipping (20–30°) thrust ramp of the Chelungpu fault (Chiu, 1971; Kao and Chen, 2000; Wang *et al.*, 2002). The earthquake ruptures show complex structural and stratigraphic relationships that can be divided into two segments: the Shihkang and Chelungpu faults. The Shihkang fault occurs within Pliocene shale and is interpreted as a bed-parallel slip fault. The Chelungpu fault of the southern segment thrust is late Pliocene shale over Quaternary fluvial deposits in the footwall.

In this study, several excavations have been carried out along the Chelungpu fault across the fault trace (Fig. 1); the excavations showed complicated structural features within unconsolidated sediments, including a ductile deformation zone at the fault tip. Because offset measurements within the ductile deformation zone are too variable to estimate the slip, in this study, we attempted other methods to estimate a relatively complete

displacement for the thrusting through more detailed observation and discussion of the characteristics of the fault-tip deformation. Here, we also present the results of our paleoseismic studies of the Chelungpu fault to assess the timing, offset, and slip rate of each event. Because active thrust faults commonly show complex geometric patterns of faulting and folding, we present a few examples of excavation that document different styles of surface faulting. We focus on the contribution of the excavation study in providing some information about fault behavior and coseismic fault-tip deformation patterns and in deriving the growth history of the fault-tip fold.
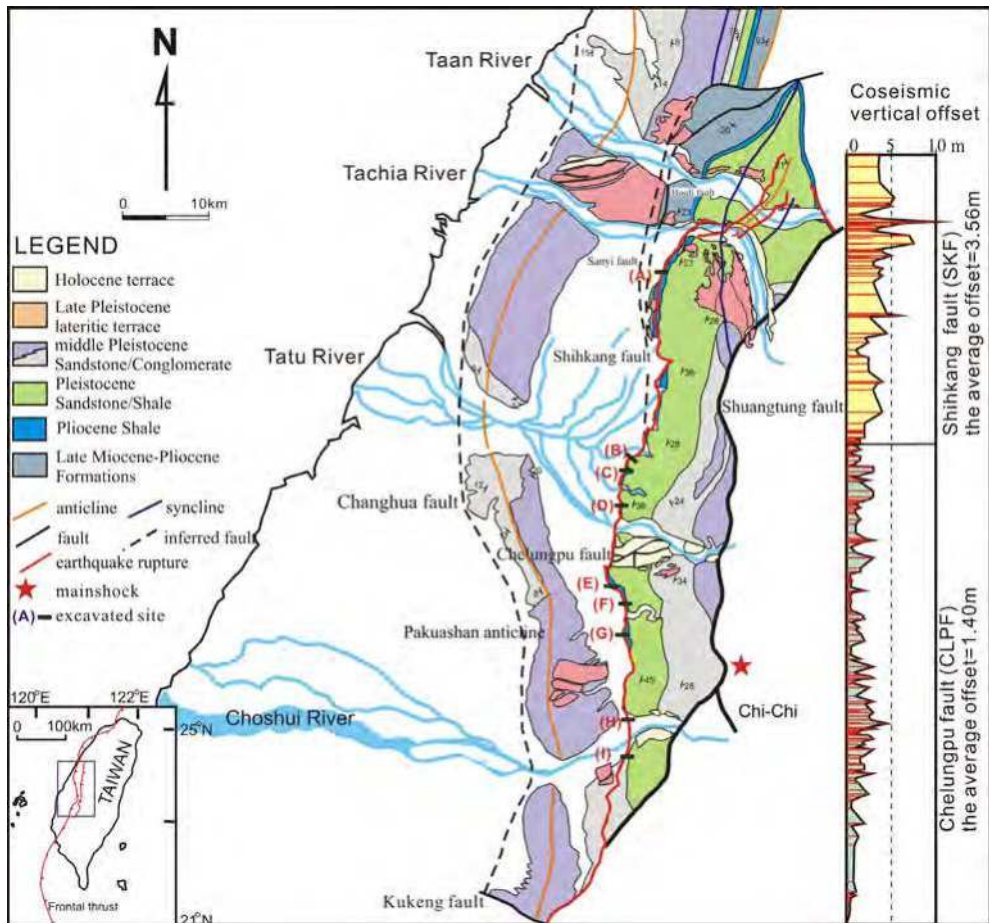

Fig. 1. Geologic map and location of the excavated sites (A-I). The Chi-Chi earthquake rupture is subdivided into the Shihkang and Chelungpu faults along the frontal Western Foothills. (A) the Fengyuan site, (B) the Wenshan farm site, (C) the Pineapple-field site, (D) the Siangong-temple site, (E) the Tsaotun site, (F) the Wanfung site, (G) the Shijia site, (H) the Mingjian site, and (I) the Chushan site. Average vertical displacement of the Chi-Chi earthquake rupture is calculated from the measured vertical displacements measured at 210 locations along the earthquake rupture.

2. The 1999 Chi-Chi earthquake ruptures

The Western Foothills in western Taiwan consist of a series of west-verging subparallel thrusts and fault-related fold structures, which have been a zone of active folding and thrusting throughout the late Quaternary (Suppe, 1981). The Chi-Chi earthquake exhibits a fault-bend fold geometry, forming a flat-ramp structure on the frontal upthrown block of the Western Foothills (Yue *et al.*, 2005; Lai *et al.*, 2006); the concealed Changhua fault of a fault propagation fold that forms the Paukashan anticline in the western side of the earthquake rupture (Fig. 1). The earthquake ruptures have complex structural and stratigraphic characteristics and can be split into two principal segments, namely, the Shihkang and Chelungpu faults. Surface slip was greatest along the northern portion of the Shihkang fault, with a maximum observed vertical slip of 9.5 m. The Shihkang fault, which has a length of about 45 km and is confined within a Pliocene shale, is interpreted as a bed-parallel slip fault, based on extrapolation from the Taiwan Core Drilling Project deep borehole. The Chelungpu fault is about 55 km in length and differs from the Shihkang fault in that the Pliocene shale overthrusts a thick sequence of Quaternary deposit. The Shihkang fault consists of a N30–40°W verging oblique thrust with vertical offsets ranging from 3–9.5 m, while the Chelungpu fault is made up of a N70–90°W verging pure thrust with vertical offsets ranging from 0.2–4 m. According to the seismicity, GPS, and SPOT data, the coseismic deformation also defines two different structural domains (Dominguez *et al.*, 2003; Pathier *et al.*, 2003; Cattin *et al.*, 2004).

3. Paleoseismologic analysis

Although the Taiwan seismic catalogs provide a historical record of strong earthquakes over the past three centuries, there is no record of any large earthquake associated with the Shihkang-Chelungpu fault (Chen *et al.*, 2004). Paleoseismic study is one of the best methods for characterizing the earthquake behavior along the Shihkang-Chelungpu fault. Over the past ten years, we have excavated numerous sites and continuously cored borings on the Chelungpu fault, where the surface rupture shows surface deformation within the Holocene deposits; our results have provided quantitative data for late Holocene slip rates (Fig. 1; Chen *et al.*, 2001a, b, 2004, 2007a, b; Ota *et al.*, 2001, 2005; Streig *et al.*, 2007). Bedrock exposed along the Shihkang fault has not been characterized in previous paleoseismic studies. Here, we integrate paleoseismologic data derived from four excavations of the Shijia, Siangong-temple, Pineapple-field, and Chushan sites to understand the characteristics of coseismic deformation of the Chelungpu fault.

3.1 Shijia site

The Shijia site is located along the frontal foothills; the surface features of the site before the earthquake show a gently alluvial fan slope of approximately 3°, which was an undeveloped terrace scarp. The 1999 fault runs along the fan slope with a hangingwall uplift of gently dipping coseismic fold scarps that are about 1 to 2 m higher than those of the footwall. We excavated a 7-m-deep, 27-m-long trench across the coseismic fold scarp formed during the Chi-Chi earthquake. The excavation showed clear exposures of well-sorted silty sand interbedded with mud and humic soil; these exposures represent overbank deposits. The exposures show three depositional units of silty sand layers (cw1, cw2, and cw3) which are

defined by the onlap of H1 and H2 humic soils (Fig. 2). The upper sequence includes two wedge-shaped deposits of cw1 and cw2 units associated with deposition across the scarp; these deposits are defined by the onlap of H1 and H2 humic soils across the forelimb. The onlapped relation indicates the occurrence of two folding events after the deposition of the H1 and H2 humic soils (Fig. 2). Detrital charcoal that was collected from the alluvial
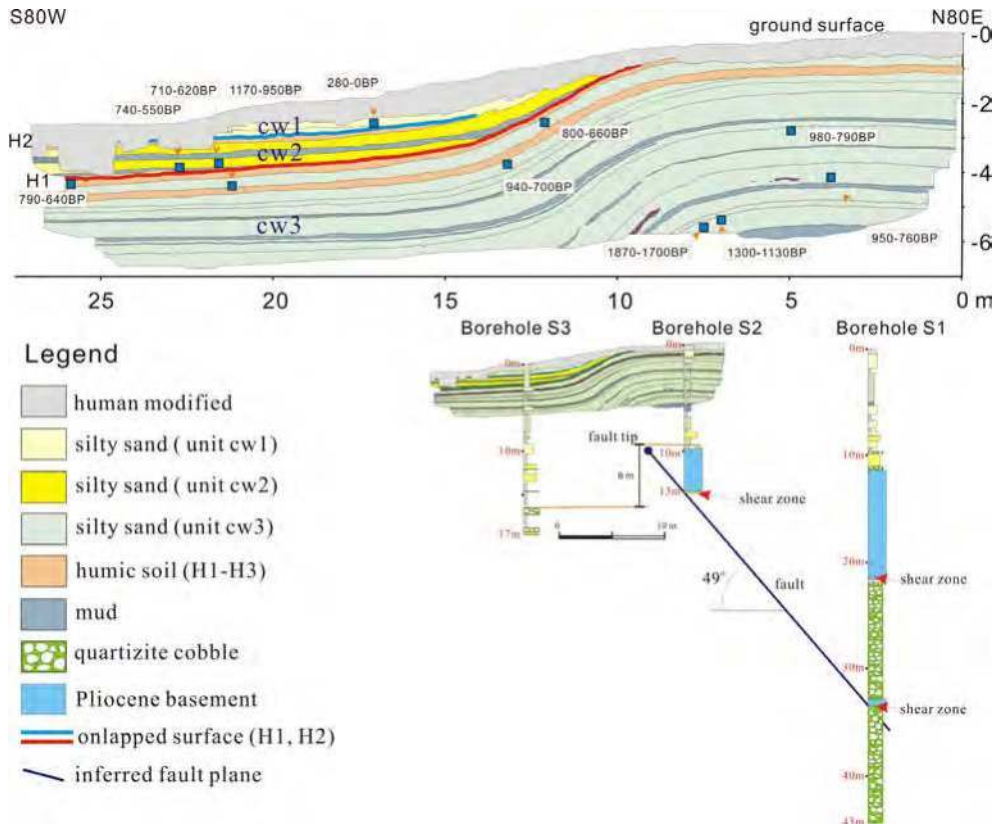

Fig. 2. The contact of alluvial deposits and humic soil (H1 and H2) occurs a distinct onlapped structure interpreted to represent a paleoearthquake event. Radiocarbon dates are used to constrain the timing of S1 and S2 paleoseismic events. Fault dip of fault depends on correlation between the borehole S1 and S2 of 49° dips. The Pliocene formation shows inclined bedding plane and is weakly sheared. The fluvial cobble deposits between boreholes S2 and S3 offset about 6-m high in both sides of the fold scarp.

deposits yields eleven radiocarbon ages; the upper part of cw3 unit: 800–660 yr BP and 940–700 yr BP, thus indicating the depositional age of 940–660 yr BP; cw2 unit: 790–640 yr BP, 740–550 yr BP, and 710–620 yr BP, indicating the depositional age of 790–550 yr BP; cw1 unit: 280–0 yr BP (Chen *et al.*, 2007b).

Borehole S1 and S2, which were drilled on the hangingwall, showed the location of the fault zone at a depth of 20.7 m and 30 m in borehole S1 and 13 m in borehole S2, where Pliocene shale is displaced over gravel deposits (Fig. 2). Based on the depth of the shear zones in both the boreholes and location of fold scarp in the excavated exposures, the fault must dip about 49° along the shallowest portion of the thrust ramp (Fig. 2). The S2 and S3 borehole logging of the top of gravel bed on both sides of the main thrust reveal a total vertical offset of 6 m, indicating that repeated large earthquakes have occurred. However, based on onlapping feature of H1 and H2 humic soils and wedge-shaped deposits of cw1 and cw2 units, we can identify two paleoearthquake events which occurred at >280 yr BP (S1 event) and 790–680 yr BP (S2 event).

3.2 Siangong-temple site

The earthquake ruptures cut through the foot of an alluvial fan and produced a gentle 1-m-high monoclinal scarp of approximately 11°. The pre-existing ground surface exhibits a gentle westward-dipping slope of approximately 2°. We excavated a 4- to 6-m-deep, 38-m-long trench across the earthquake scarp; the excavation exposed six wedge-shaped alluvial units: aw1, aw2, aw3, aw4, aw5, and aw6 (Fig. 3). A distinctive humic soil overprints the top of each colluvial unit, which consists of a well-sorted sand layer with a channelized gravel bed. The wedge-shaped colluvial deposits were well-defined by Os1, Os2, Os3, Os4, and Os5 humic soils, which were unconformably overlain by colluvial deposits after a large earthquake. Unit aw2, for example, pinched out over the Os3 soil of the forelimb or was eroded on the uplifted side of the fold crest. However, based on onlapping relations, it was deduced that the colluvium was deposited across the forelimb of a coseismic fold scarp and that at times, the colluvium onlapped and overlapped against the forelimb. The dips of soil in the forelimb progressively decrease toward the ground surface from 38° (Os5) to 11° for the Chi-Chi earthquake-induced slope (Fig. 3). Upward change in dips, hindward thinning, and angular unconformites between soils and overlying colluvium are interpreted as indicating the occurrence of repeated large earthquakes on the Chelungpu fault. The radiocarbon ages obtained from detrital charcoal that was collected from units aw1, upper aw4, lower aw4, and aw5 are <300 yr BP, 1960–1810 yr BP, 3000–2840 yr BP, and 3100–2920 yr BP, respectively.

Boreholes T1 and T2 were drilled to a depth of 40 m on the hangingwall and to a depth of 50 m on the footwall. Borehole T1 constrains the location of the fault zone at a depth of 22.8 m between the Pliocene shale and Holocene colluvial deposits. We link the fault zones in borehole T1 and the synclinal fold axis in the excavated exposures; the results suggest a 30° east-dipping blind fault (Fig. 3). A corresponding gravel bed between boreholes T1 and T2 is offset to a height of 40 m on both sides of the fold scarp, indicating that several large earthquakes have occurred. Based on the syntectonic sedimentary structure, we infer that five paleoearthquake events including the Chi-Chi earthquake occurred near 1960–1810 yr BP (G3 event) and 3160–2840 yr BP (G4 event); however, we have not been able to obtain age control for the G1 and G2 events (Chen *et al.*, 2007b).
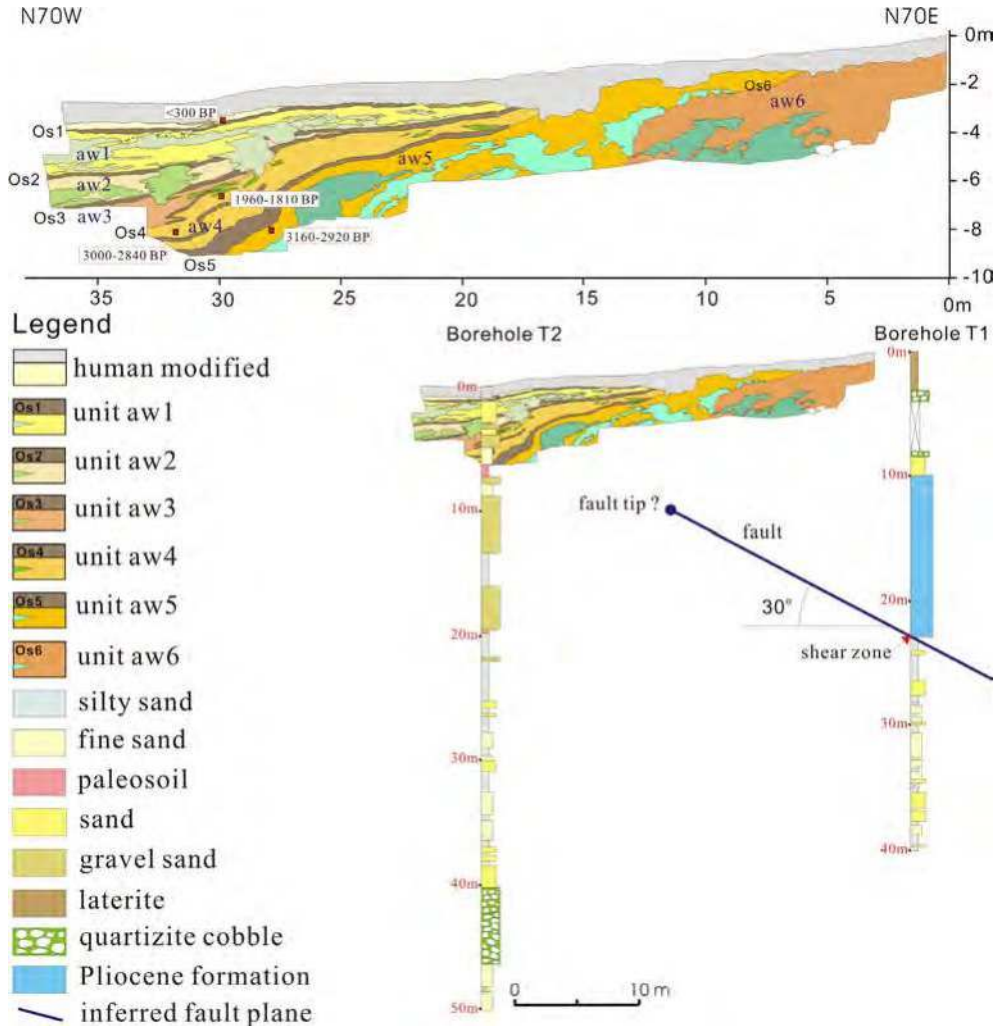
Fig. 3. Sketch of trench-wall emphasizing the top of beds of soil (Os) and gravel depositional wedges (aw). Alluvial gravels onlap onto each soil bed forming a wedge-shaped depositional unit. Borehole T1 reveals a shear zone at the bottom of Pliocene formation which shows inclined bed and slightly shearing at the excavated site. Correlation with a shear zone at depth in the borehole T1 and the synclinal fold axis in the excavated exposures identifies a fault-plane dipping of 30°.

3.3 Pineapple-field site

Repeated coseismic displacements show clear morphological expressions on both sides of the fault zone; the expressions commonly occur as a lineament scarp between the foothills and the basin plain (Chen *et al.*, 2003). The site was dug across a pre-existing terrace scarp, where the earthquake rupture clearly uplifted the hangingwall by about 1.6–2.1 m. We
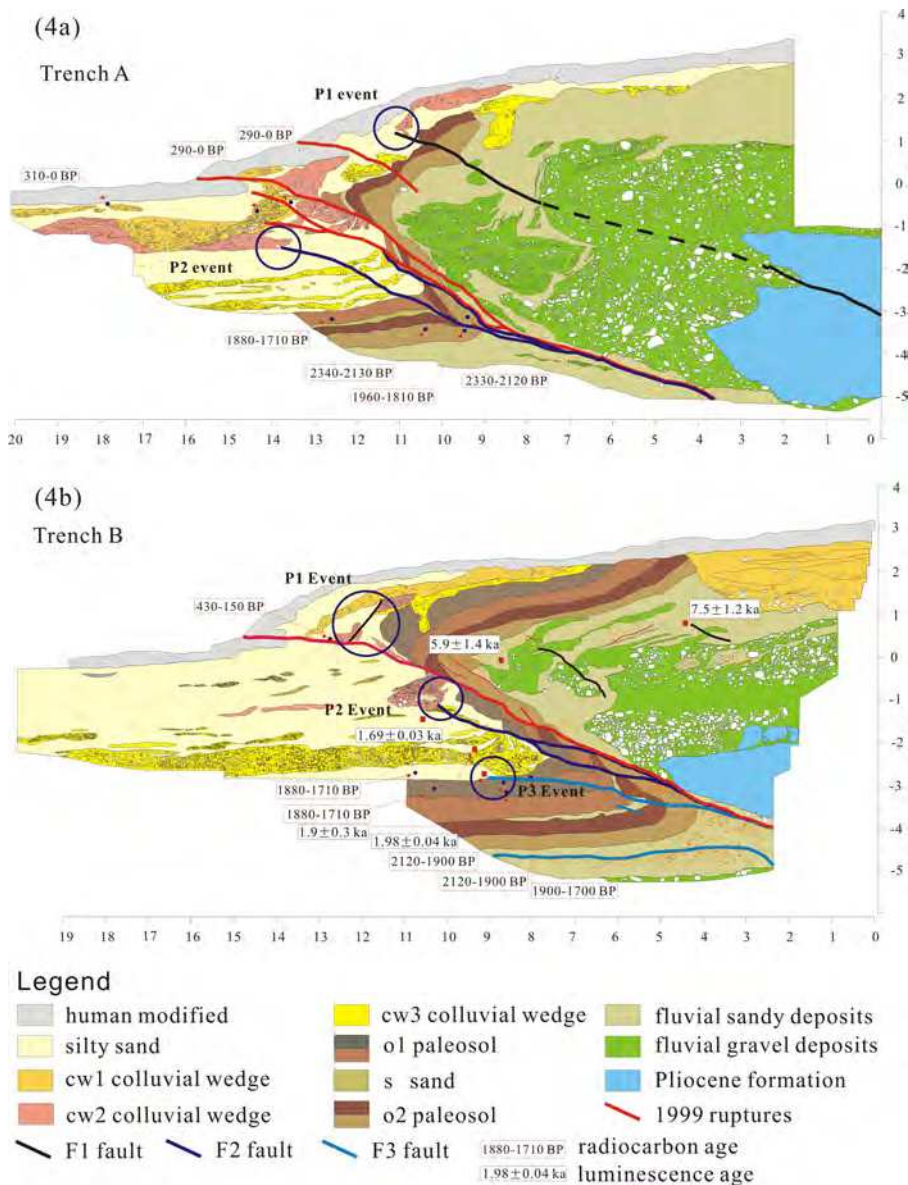
Fig. 4. (a, b) Five types of deposits, the 1999 earthquake ruptures, and three paleo-coseismic faults (F1, F2, and F3) are observed in the excavation of the Pineapple-field sites. The Pliocene basement is overthrust on the hangingwall. The older sediments of the fluvial gravel deposits reached at 2 m depth on the hangingwall and 5 m depth on the footwall. The fluvial gravel deposits have 6 m vertical offset across the main fault. The top soil is offset 1.6 m at trench A (Fig. 4a) and 2.1 m at trench B (Fig. 4b) in both sides of the 1999 earthquake ruptures. Radiocarbon dates are used to constrain the timing of P1, P2, and P2 paleoseismic events.

excavated a 25-m-long, 8-m-deep trench, which showed clear exposures of the Pliocene rock, Holocene fluvial, and colluvial deposits. The Pliocene basement is preserved on the upthrown block, which is unconformably covered by Holocene fluvial gravel and boulder beds (Figs. 4a and 4b). The downthrown block is deposited by Holocene fluvial deposits of soils (s1 and s2 units), and sand layers are interbedded with colluvial wedge-shaped gravel beds (cw1, cw2, and cw3 units). Wedge-shaped colluvium overlies the paleoearthquake ruptures, indicating that the colluvium evidently represents the earthquake-induced deposits.

The excavation at the Pineapple-field site indicates several shear planes including the Chi-Chi earthquake and other paleoearthquake ruptures. The character deformation at the fault front indicates ductile deformation comprising a hangingwall anticline and a footwall syncline with an overturned limb and increasing thickness in the anticlinal hinge. The Chi-Chi earthquake rupture here indicates a fault-bend fold geometry, forming a flat-ramp structure cutting through the ground surface. The ruptures branch into several reverse faults, which form about N42^{o}E trending and a 26° southeast-dipping fault. The excavation exposes three paleoearthquake thrust faults, namely, F1, F2, and F3, which are defined by a wide thrust zone with fully developed thin shear bands (Figs. 4a and 4b).

Luminescence dating constrains the age of the top layer of alluvial deposits (f unit) to about 4 ± 0.3 ka (Chen *et al.*, 2009). Except for luminescence date, all the other twelve detrital charcoal samples collected from fluvial deposits yield radiocarbon ages as follows: s2 unit: from 2340–2130 yr BP to 1910–1810 yr BP; s1 unit: from 2120–1900 yr BP to 1880–1710 yr BP; cw3 unit: 1880–1690 yr BP; cw2 unit: < 1690 yr BP; cw1 unit: 430–150 yr BP. However, based on structural and depositional relations, it is inferred four paleoearthquake events including the Chi-Chi earthquake occurred at the Pineapple-field site. Based on the radiocarbon age constraints of the paleoearthquakes, it is inferred that the four events occurred at 430–150 yr BP (P1 event), <1690 yr BP (P2), 1900–1710 yr BP (P3 event), and the 1999 Chi-Chi earthquake (Chen *et al.*, 2004).

3.4 Chushan site

The Chushan site is located on an alluvial fan; the Chi-Chi earthquake rupture was located between this fan and the Western Foothills. We excavated an approximately southeast-trending, 35-m-long, 14-m-wide, 8-m-deep trench, which exposed two depositional sequences; these sequences represent an abrupt change in the local depositional environment from fluvial to alluvial fans (Figs. 5a and 5b). The lower sequence of thick-bedded boulder beds represents fluvial deposition. The upper sequence is divided into six units (units A–F) comprising sand with lenticular gravel beds and silt with thin mud based on their distinctive lithologies, which the alluvial deposits derived from the hangingwall strata of the Western Foothills.

The Chi-Chi earthquake rupture produced a 1.7-m-high vertical offset and about 3.5 m of horizontal shortening on an east-dipping fault with thrust displacement that is oriented 32° in the south wall and 20–24° in the north wall. The excavation shows that fault-tip deformation can be subdivided into breakthrough fault-propagation and fault-bend folds. Fault-tip deformation in the south wall, which is the main fault that cuts through the ground surface, is exposed as a fault-bend fold with an asymmetric anticlinal fold and a ramp-flat thrust (Fig. 5a). On the north wall of the excavation, the folding style is similar to a fault-propagation fold, and the tip of the main fault cuts through the ground surface during the Chi-Chi earthquake (Fig. 5b). A ductile shear zone near the ramp thrust forms rollover folds that show an overturned forelimb on the hangingwall.

Legend

Backfills (S)   Sand with lenticular gravel layer (A)   Humic soil (B)   Silt layer (B)   Silty mud (C)

Silt with thin mud (D)   Mud with thin sand (E)   Sand with lenticular gravels (F)

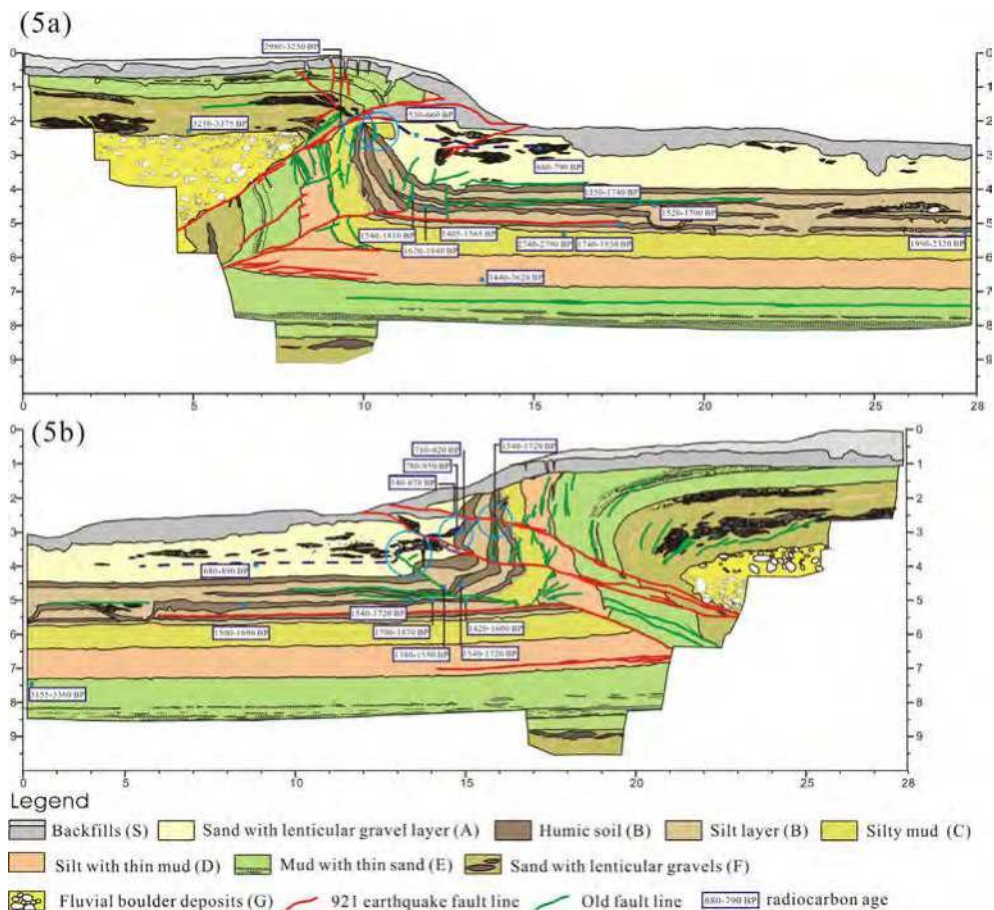Fluvial boulder deposits (G)   921 earthquake fault line   Old fault line   680-790 BP radiocarbon age

Fig. 5. (a) The south wall of the Chushan excavation shows a breakthrough thrust fault, where the tip of the thrust ramp follows the anticlinal axial surface. The fault tip deformation causes a fault-bend fold, forming a broadly open anticline and a ramp-flat thrust. (b) The north wall of the Chushan excavation shows a breakthrough fault-propagation folding geometry, which contains a recumbent anticline with an overturned forelimb. Radiocarbon dates are used to constrain the timing of stratigraphic units.

In borehole C1 on the hangingwall, the fault zone is located at a depth of 54.3 m, where Pliocene shale is displaced over Holocene deposits. We link the fault zones in boreholes C1 and the synclinal fold axis in the excavated exposures; the results suggest a fault with a dip of 24°, which is consistent with the measurement of the fault plane of about 20–32° in the excavation. A corresponding gravel bed between borehole C2 and the excavation on the hangingwall is offset to a height of 7 m on both sides of the main fault, indicating that repeated large earthquakes have occurred.

One wood sample that was collected from fluvial terrace deposits near the excavated site and interpreted to be correlative with unit G yielded a radiocarbon age of 3470–3820 yr BP (Figs. 5a and 5b). All of the 26 detrital charcoal samples collected from the upper sequence

of fluvial deposits and divided into six units (units A–F) yield radiocarbon ages as follows: F unit: 3380–2980 yr BP; E unit: 3360–3155 yr BP; C unit: 2790–2740 yr BP; B4 subunit: 2320–1740 yr BP; B3 subunit: 1710–1540 yr BP; B2 subunit: 1700–1550 yr BP; B1 subunit: 1550–710 yr BP (the top of soil: 950–710 yr BP); lower A unit: 890–680 yr BP; upper A unit: 670–530 yr BP. The timing of the paleoearthquake events can be deduced from the observed earthquake-induced wedge-shaped colluvium, progressive fault displacements on the stratigraphic units, and fault intersections and terminations. However, based on structural and depositional relations, it is inferred that five paleoearthquake events including the Chi-Chi earthquake occurred at the Chushan site at 790–680 yr BP (C1 event), 950–790 yr BP (C2 event), 1550–1380 yr BP (C3 event), and 1930–1710 yr BP (C4 event) (Chen *et al*., 2007a).

4. Discussion

Repeated coseismic displacements commonly show tectonic-geomorphic features related to displace Holocene sediments, which form a fault or a fold scarp, but it was difficult to determine the related fault or fold. Active thrust faults commonly show complex geometric patterns of faulting and folding in response to different sedimentary facies, thickness, and lithologic characters of Holocene deposits. Previous studies along the Chi-Chi earthquake rupture have shown that fault-tip deformation can be subdivided into breakthrough thrust and blind-thrust components (Chen *et al*., 2001a, b, 2004, 2007a, b; Ota *et al*., 2001, 2005; Streig *et al*., 2007). We will integrate these excavated profiles across the earthquake rupture to delineate the characteristics of thrust-related fold and to reconstruct the growth history of the fault tip fold. Moreover, evidences for repeated coseismic deformation can be identified by relationships between the structural and sedimentological features, such as colluvial wedges, unconformity, and onlap and overlap geometries. We will exploit these types of relationships to characterize the surface deformation that is associated with the sedimentary features. Therefore, in the following, we present the observation of deformation geometries that document the fault-propagation fold of the Shijia and Siangong-temple sites, breakthrough fault-propagation fold of the Pineapple-field site and the north wall of the Chushan site, and fault-bend fold of the south wall of the Chushan site.

4.1 Fault-propagation fold

The Shijia and Siangong-temple excavations show a monoclinal fold that produced a gentle fold scarp, where the fault tip did not propagate through the surface deposits. Coseismic uplift during the Chi-Chi earthquake produced a vertical displacement of 0.8 m at both sites, which is less than the average vertical offset of about 1.4 m along the Chelungpu fault. The excavated exposures reveal a structural complexity resulting from ductile deformation, which makes it difficult to account for the complete deformation field associated with each coseismic event. The trishear model provides an important alternative to restore deformation for a fault-propagation fold that exhibits fault-tip ductile deformation within folded strata (Erslev, 1991; Hardy and Ford, 1997).

The Shijia and Siangong-temple excavations indicate that the cohesive strength of sediments is low, which apparently allows trishear deformation within the folded strata in the shallow subsurface. The main focus of this study is to understand coseismic growth folding characters across a monoclinal fold above a trishear deformation zone. The excavation shows several alluvial units that onlap soil layers on the forelimb of a monoclinal fold. The thickness of each alluvial deposit gradually decreases across the forelimb, forming wedge-

shaped deposits, which were laid to onlap and overlap the forelimb. The wedge-shaped bed, which represents material reworked from the hangingwall immediately after a surface-rupturing earthquake, commonly occurred at a location above an unconformity on the hangingwall. This indicates that folding produces an uplift of the fold crest and a forelimb with a large deposition on the footwall. The depositional architecture of an alluvial unit shows an aggradational forward depositional sequence on the forelimb (Figs. 6 and 7). The wedge-shaped deposits bounded by the soil layers represent the postseismic sediments, and the soils form during periods with low depositional rates, which encourage soil development (Machette *et al.*, 1992). Therefore, the wedge-shaped depositional unit brackets coseismic uplift and interseismic deposition, which provide evidence for a surface-rupturing earthquake event.
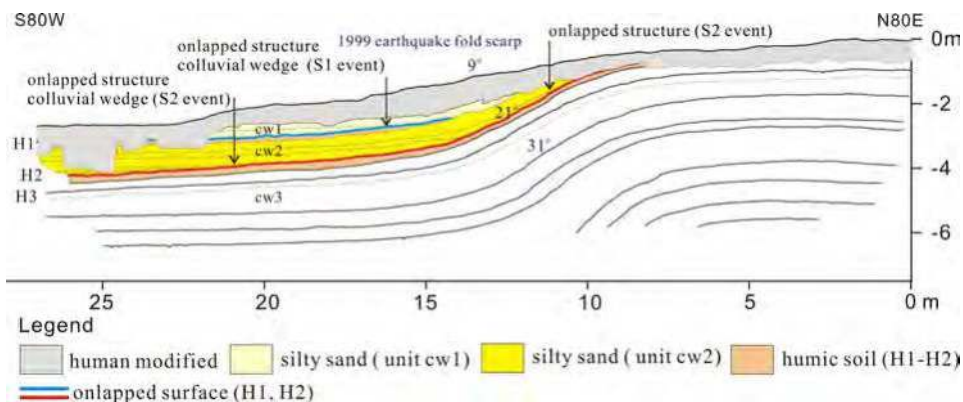

Fig. 6. The Chi-Chi earthquake formed a westward-dipping scarp dipping approximately 9°on the Shijia site. Sketch of trench-wall highlights the top of the ground surface, humic soil, and mud layers. Soil dip within the forelimb increases from 9° to 31°. The silty and sandy sediments onlap onto the H1 and H2 humic soils form a wedge-shaped alluvium.
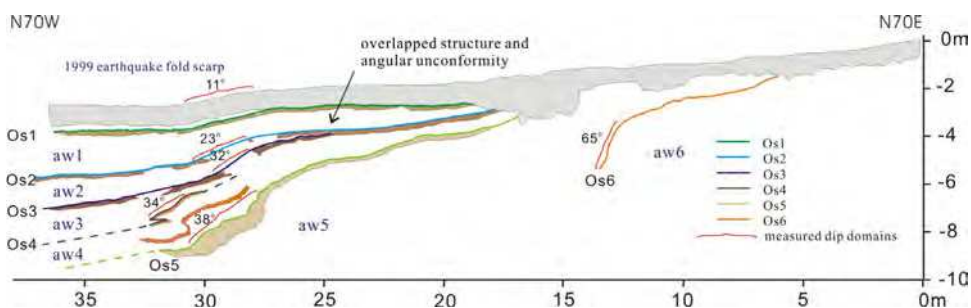

Fig. 7. Siangong-temple excavated profile shows a monoclinal fold with a gently dipping west-facing forelimb of approximately 11° that formed during the Chi-Chi earthquake. The dips of soil within the forelimb increase from 11° to 38° and show a fanning of bed dips. Soils (Os1, Os2, Os3, Os4, and Os5) can provide useful controls on the interpretation of trench stratigraphy which bound five alluvial wedges (aw1, aw2, aw3, aw4, and aw5) representing several episodic seismic events.

Based on structural and depositional relations in excavated exposures, it is inferred that the Shijia and Siangong-temple sites show a progressive fanning and an increase in dips for soils of low stratigraphic units, which is consistent with growth strata geometries of the trishear deformation model (Erslev, 1991; Hardy and Ford, 1997; Allmendinger, 1998). Growth strata show the progressive tilted forelimb of the monoclinal fold that is caused by changes in the dip during the earthquake event. In addition, fanning of the soil dip within the forelimb indicates that the monoclinal fold grew by repeated coseismic deformation. At the Shijia site, strata of backfills and H1 and H2 soils above the forelimb show an increase in the dip of 9°, 21°, and 31°, respectively, which represent three paleoearthquake events including the Chi-Chi earthquake (Fig. 6). The Siangong-temple site also shows fanning of the soil dip within the forelimb, this indicates an increase in the dip of 11°, 23°, 32°, 34°, and 38°, which represent four paleoearthquake events including the Chi-Chi earthquake (Fig. 7). The growth fault-propagation fold in the excavation showed growth folding characters that revealed at onlap and overlap features, unconformity, fanning forelimb dip, and wedge-shaped deposits, that each wedged depositional unit in the Siangong-temple and Shijia sites respectively represents a surface-rupturing paleoearthquake event.

4.2 Breakthrough fault-propagation fold

The geomorphologic features of the Pineapple-field and Chushan sites show a visible fold scarp where the Chi-Chi earthquake rupture followed the pre-existing Holocene scarp. The geomorphologic evidence indicates that the observable vertical separation of terrace scarps may have been produced by several paleoearthquakes along the toe of scarp. The structural characteristics obtained during excavation at the two sites indicate breakthrough faulting, which occurs when the fault-tip deformation causes a fault-bend fold and a breakthrough fault-propagation fold. The Pineapple-field excavation (Figs. 8a and 8b) and the north wall of the Chushan excavation (Fig. 9a) show a breakthrough fault-propagation folding geometry. The two excavations contain a recumbent anticline with an overturned forelimb, which yields a tightly anticlinal hinge with bed thickening, and a steeply narrow forelimb with pronounced bed thinning. The forelimb is dominated by flexural slip within the deformation zone owing to fold-forward rotation. We interpret the deformation within the forelimb as being the product of hangingwall strata rolling into the deformation zone, which resulted in the growth of numerous layer-parallel slip shear planes. The forelimb may increase in length owing to hinge migration and limb rotation (Mitra, 2002). Hence, the bedding slip indicates that the overall deformations may have been quite large in the forelimb. Though the main fault tip breaks through the ground surface at the Pineapple-field excavation and the north wall of the Chushan excavation during the Chi-Chi earthquake, the fault tip of the main thrust faults occurred slip displacement of 1.2–1.8 m and 1.5 m less than that toward the lower reaches displacement of 4.2 m and 3.8 m, respectively. The displacement along the fault reaches found here seem to be consistent with that obtained using the trishear model of displacement variations, in which the amount of slip along the fault near the surface is much less than that toward the lower reaches (Erslev, 1991). Therefore, it is difficult to obtain the actual displacement at the fault tip within the trishear zone. However, the structural relief on the hangingwall is equal to the vertical displacement along the lower reaches of the fault beyond the trishear zone. Outside of the trishear zone, the actual slip on the upthrown block can be determined from the structural

relief and dip of the fault. For these reasons, the deformation of the breakthrough fault-propagation fold is studies by focusing on the measurement of the vertical displacement on the hangingwall away from the trishear zone, which produces reliable measurements for the estimation of the actual displacement.
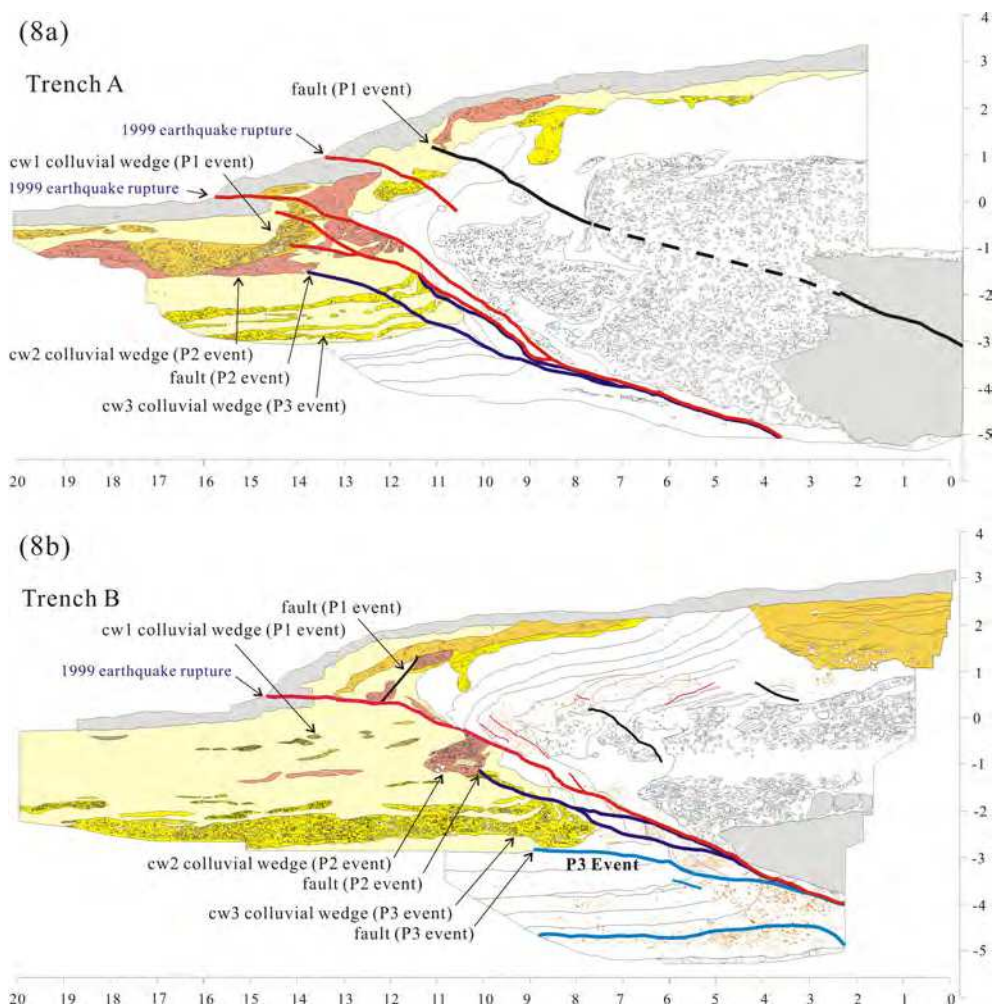

Fig. 8. The structural and stratigraphic features of the earthquake rupture on the A profile (8a) and B profile (8b) of the Pineapple-field site. The colored pattern of stratigraphic units shows the wedge-shaped colluvial deposits. The structural and stratigraphic features also show onlapped features and colluvial wedges that inferred the P1, P2 and P3 paleoearthquake events.
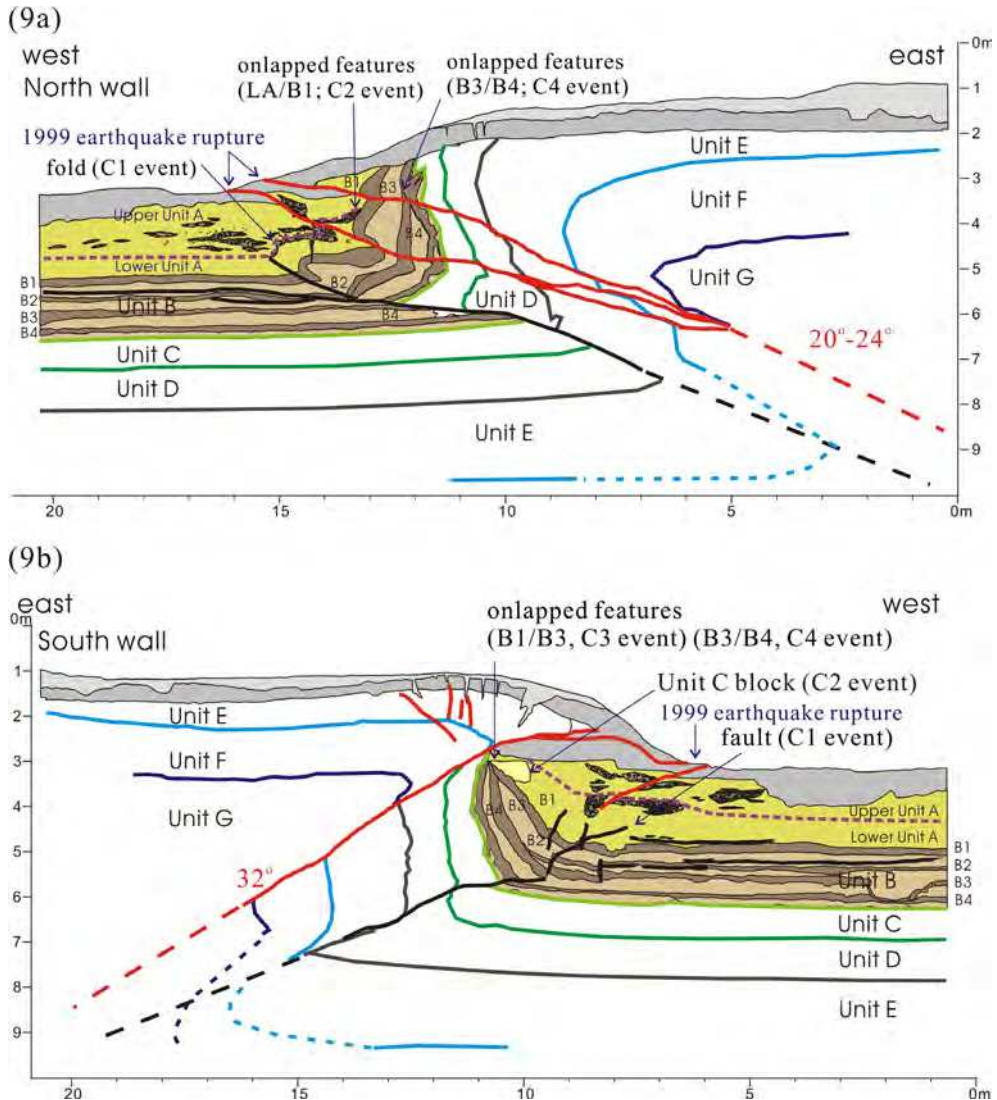
Fig. 9. The structural and stratigraphic features of the earthquake rupture on the north wall (9a) and south wall (9b) of the Chushan site. The red lines show the Chi-Chi earthquake fault strands. The black lines show the paleoearthquake fault strands. The colored pattern of stratigraphic units shows the wedge-shaped colluvial deposits. The structural and stratigraphic features also show folded and onlapped features that inferred the C1, C2, C3, and C4 paleoearthquake events.

4.3 Fault-bend fold

The south wall of the Chushan excavation is found to be a breakthrough thrust fault, where the tip of the thrust ramp follows the anticlinal axial surface, showing a clear displacement

along the fault ramp. The fault-tip deformation causes a fault-bend fold, forming a broadly open anticline and a ramp-flat thrust. The anticline on the frontal upthrown block produced by the Chi-Chi earthquake is associated with a minor west-dipping backthrust, tensile cracks, and normal faults at the anticline crest along a main east-dipping 32° breakthrough thrust (Fig. 9b). A footwall syncline is found to have produced a thinning and oversteepened forelimb due to the shearing and dragging produced by the repeated paleoearthquakes. The synclinal forelimb below the fault ramp is defined by a 2-m-wide deformation zone with numerous thin shear planes. The unfolded strata on the hangingwall suggest that the fault tip broke through the ground surface at an earlier stage, even as the fault continued to propagate and the footwall continued to fold; this suggests a hangingwall-fixed fault-bend folding mechanism. However, the fault-bend fold associated with a steep ramp in the underlying thrust propagated through the unfolded strata on the upthrown block. The slip along the thrust may be transferred with an equal displacement during the coseismic deformation. For this calculation, the actual slip on the upthrown block can be determined from the structural relief and dip of the fault.
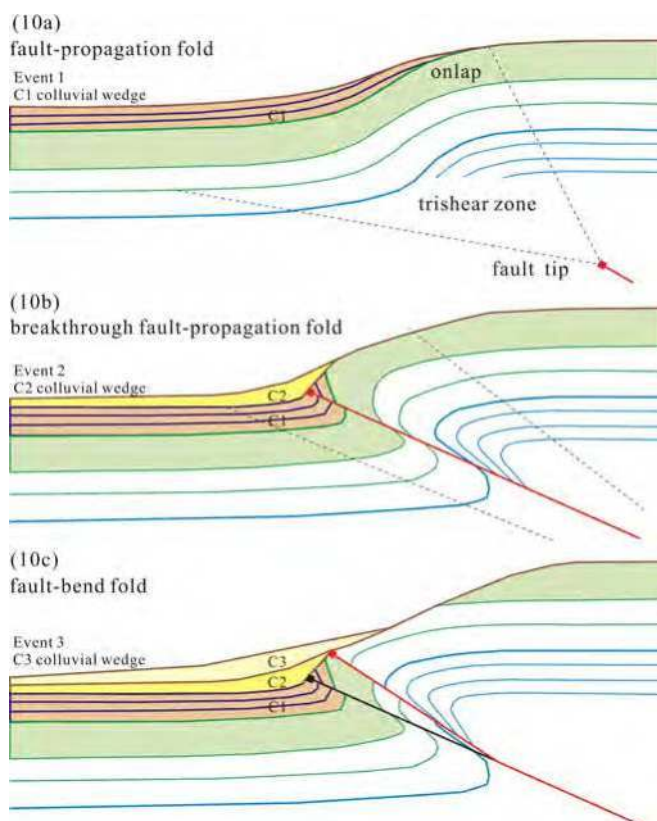

Fig. 10. Sketch diagrams of the structural and stratigraphic features show that the evolutionary path of thrust-related folds in the excavation develops from fault-propagation folding to breakthrough fault-propagation folding and finally to fault-bend folding.
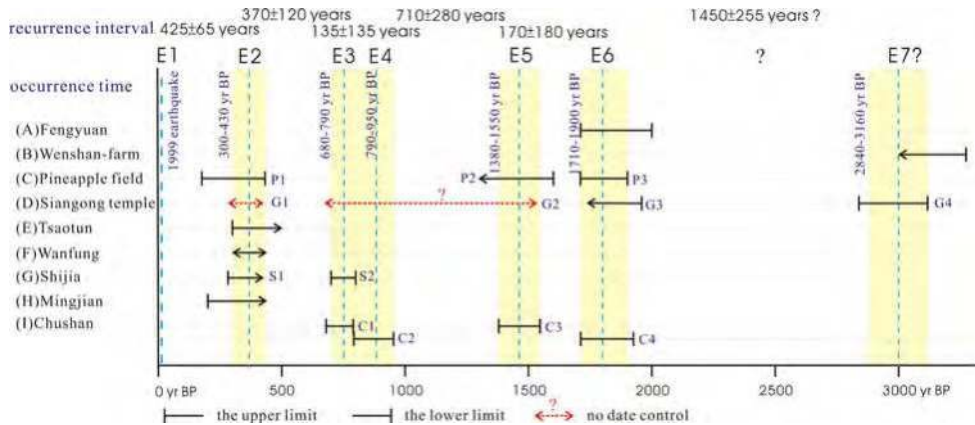
Fig. 11. Correlation between earthquake events at nine excavated sites on the Shihkang and Chelungpu faults, showing occurrence time and recurrence interval. The occurrence time estimates corresponds to the color rectangles based on radiocarbon dating. The horizontal black lines indicate the age range for each event at each site. Lines terminated by vertical bars have defined upper or lower age limits; arrowheads indicate undetermined limits. The locations of excavation sites (A-I) are shown in Figure 1.

Our analysis of the configuration of paleoseismic excavations along the 1999 Chi-Chi earthquake rupture identified three structural features of the fault tip deformation associated with thrust-related folding, suggesting that the evolutionary path of thrust-related folds in the excavation develops from fault-propagation folding to breakthrough fault-propagation folding and finally to fault-bend folding (Fig. 10). Stage I. The structural configuration of the Shijia and Siangong-temple excavations is interpreted to be the product of a monoclinal fold above the blind thrust fault during the earliest part of thrust-related fold development; this indicates the formation of a growth fault-propagation fold based on the trishear deformation model (Fig. 10a). The folding characters reveal onlap and overlap geometries, unconformity, fanning forelimb dip, and wedge-shaped deposits; each wedged depositional unit represents a surface-rupturing paleoearthquake event. Stage II. The structural configuration of the Pineapple-field excavation and the north wall of the Chushan excavation is interpreted to be a breakthrough fault-propagation fold showing a recumbent anticline with an overturned forelimb. The advancing thrust fault is found to have broken through the ground surface, and the continuing fault propagation rotates the forelimb in both the hangingwall and footwall. The folding characters yield a tightly folded hinge, a steep and narrow folded forelimb with pronounced bed thinning, and an anticlinal hinge with bed thickening (Fig. 10b). Stage III. The structural configuration of the south wall of the Chushan excavation is interpreted to be a fault-bend fold. The tip of the main thrust fault breaks through the anticlinal hinge, forming a hangingwall-fixed fold (Fig. 10c).

Over the past tens years, we have excavated numerous trenches on the Chelungpu fault, where the surface rupture shows surface deformation within the Holocene deposits (Fig. 1). Here, we integrate paleoseismologic data with the data derived from excavations to understand the behavior of the Chelungpu fault. By excavating numerous sites along the strike of the Chelungpu fault, we document six surface-rupturing events that have occurred over the last 2000 years. These are the events that occurred in 1999 A.D. (E1), 430–300 yr BP (E2), 790–680 yr BP (E3), 950–790 yr BP (E4), 1550–1380 yr BP (E5), 1900–1710 yr BP (E6), and

3160–2840 yr BP (E7?), respectively (Fig. 11). The E1, E2, E3, and E6 events were well exposed in most excavations and are extremely well-resolved events. The E4 and E5 events have been documented only at the Chushan site in the southernmost part of the Chelungpu fault. The paleoseismic data allow us to define recurrence intervals of 425±65, 370±120, 135±135, 710±280, and 170±180 years along the Chelungpu fault. The recurrence intervals have not been uniform over the past two millennia (Fig. 11). The data from individual paleoseismic sites indicate that the dip slip rate ranges from 4.2 to 9.6 mm/yr.

5. Conclusions

The deformed configuration at the fault tip, resulting from the four excavated sites along the 1999 Chi-Chi earthquake rupture, showed three geometric patterns: fault-propagation, breakthrough fault-propagation, and fault-bend folds. The development deformation is modified by subsequent translation on the propagating fault tip. During the initial deformation, the thrust fault propagates upward through the undeformed units, producing a fault-propagation fold. Then, the fault tip breaks through the ground surface, resulting in a transition from breakthrough fault-propagation folding to fault-bend folding.

The paleoearthquake events are determined by radiocarbon dating of wedge-shaped colluvial deposits exposed in trenches. Evidence obtained from excavation across the Chi-Chi earthquake rupture indicates that there have been six large earthquake events during the past two millennia, which occurred in 1999 A.D. (E1), 430–300 yr BP (E2), 790–680 yr BP (E3), 950–790 yr BP (E4), 1550–1380 yr BP (E5), and 1900–1710 yr BP (E6), suggesting relatively short recurrence intervals in the order of 150–700 years.

6. References

Allmendinger, R.W. (1998) Inverse and forward numerical modeling of trishear fault-propagation folds, *Tectonics* 17, 640–656.

Cattin, R., Loevenbruck, A., Le Pichon, X. (2004) Why does the co-seismic slip of the 1999 Chi-Chi (Taiwan) earthquake increase progressively northwestward on the plane of rupture? *Tectonophysics* 386, 67–80.

Central Geology Survey (1999) Report of the geological survey of the 1999 Chi-Chi earthquake (in Chinese), Central Geological Survey, Taipei.

Chen, W.S., Chen, Y.G., Chang, H.C. (2001a) Paleoseismic study of the Chelungpu fault in the Mingjian area, *West. Pacific Earth Sci.* 1, no. 3, 351–358.

Chen, W.S., Chen, Y.G., Chang, H.C., Lee, Y.H., Lee, C.C. (2001b) Paleoseismic study of the Chelungpu fault in the Wanfung area, *West. Pacific Earth Sci.* 1, no. 4, 43–72.

Chen, W.S., Huang, B.S., Chen, Y.G., Lee, Y.H., Yang, C.N., Lo, C.H., Chang, H.C., Sung, Q.C., Huang, N.W., Lin, C.C., Sung, S.H., Lee, K.J. (2001c) Chi-Chi earthquake, 1999 September 21: a case study on the role of thrust-ramp structures for generating earthquakes, *Bull. Seism. Soc. Am.* 91, no. 5, 986–994.

Chen, W.S., Chen, Y.G., Shih, R.C., Liu, T.K., Huang, N.W., Lin, C.C., Sung, S.H., Lee, K.J. (2003) A modern analog of the out-of sequence thrust system in relation with the Chi-Chi earthquake ruptures in the Western Foothills, central Taiwan, *J. Asian Earth Sci.* 21, 473–480.

Chen, W.S., Lee, K.J., Lee, L.S., Ponti, D.J., Prentice, C., Chen, Y.G., Chang, H.C., Lee, Y.H. (2004) Slip rate and recurrence interval of the Chelungpu fault during the past 1900 years, *Quat. Int.* 115–116, 167–176.

Chen, W.S., Yang, C.C., Yen, Y,C., Lee, L.S., Lee, K.J., Yang, H.C., Chang, H.C., Ota Y., Lin, C.W., Lin, W.H., Shih, T.S., Lu, S.T. (2007a) Late Holocene paleoseismicity of the southern portion of the Chelungpu fault, central Taiwan: Evidence from the Chushan excavation site, *Bull. Seism. Soc. Am.,* 97(1B), 1–13.

Chen, W.S., Lee, K.J., Lee, L.S., Streig, A.R., Chang, H.C., Lin, C.W. (2007b) Paleoseismic evidence for coseismic growth-fold in the 1999 Chichi earthquake and earlier earthquakes, central Taiwan, *J. Asian Earth Sci.* 31, 204–213.

Chen, Y.G., Chen, Y.M., Chen W.S., Lee, K.J., Lee, L.S., Lu, S.T., Lee, Y.H., Watanuki, T., Lin, Y.N. (2009) Optical dating of a sedimentary sequence in a trenching site on the source fault of the 1999 Chi-Chi earthquake, Taiwan, *Quat. Int.* 199, 25–33.

Chiu, H.T. (1971) Folds in the Northern Half of Western Taiwan, *Petrol. Geol. Taiwan* 8, 7–19.

Dominguez, S., Avouac, J.P., Michel, R. (2003) Horizontal coseismic deformation of the 1999 Chi-Chi earthquake measured from SPOT satellite images: Implications for the seismic cycle along the western foothills of central Taiwan, *J. Geophy. Res.* 108, no. B2, 2083, doi:10.1029/2001JB000951

Erslev, E.A. (1991) Trishear fault-propagation folding, *Geology* 19, 617–620.

Hardy, S., Ford, M. (1997) Numerical modeling of trishear fault-propagation folding, *Tectonics* 16, 841–854.

Kao, H., and W.P. Chen (2000) The Chi-Chi Earthquake sequence: active, out-of-sequence thrust faulting in Taiwan, *Science* 288, 2346–2349.

Lai, K.Y., Chen, Y.G., Hung, J.H., Suppe, J., Yue, L.F., Chen, Y.W. (2006) Surface deformation related to kink-folding above an active fault: Evidence from geomorphic features and co-seismic slips, *Quat. Int.*147, 44–54.

Machette, M.N., Personius, S.F., Nelson, A.R. (1992) Paleoseismicity of the Wasatch Fault zones: a summary of recent investigation, interpretations and conclusions, In Gori, P.L. (Ed.), Assessment of regional earthquake hazards and risk along the Wasatch Front, Utah, *U.S. Geol. Surv. Professional Paper* 1500, p. A1–A30.

Mitra, S. (2002) Fold-accommodation faults, *Am. Asso. Petrol. Geol. Bull.* 86, 4, 671–693.

Ota, Y., Huang, C.Y., Yuan, P.B., Sugiyama, Y., Lee, Y.H., Watanabe, M., Sawa, H., Yanagida, M., Sasake, S., Tanifuchi, K. (2001). Trenching study at the Tsaotun site in the central part of the Chelungpu Fault, Taiwan, *West. Pacific Earth Sci.* 1, no. 4, 487–498.

Ota. Y., Chen, Y.G., Chen, W.S. (2005) A review on paleoseismological and active fault study in Taiwan, *Tectonophysics* 408, 63–77.

Pathier, E., Fruneau, B., Deffontaines, B., Angelier, J., Chang, C.P., Yue, S.B., Lee, C.T. (2003) Coseismic displacements of the footwall of the Chelungpu fault caused by the 1999, Taiwan, Chi-Chi earthquake from InSAR and GPS data, *Earth Planet. Sci. Lett.* 212, 73–88.

Streig, A.R., Rubin, C.M., Chen, W.S., Chen, Y.G., Lee, L.S., Thompson, S., Madden, C., Lu, S.T. (2007) Evidence for prehistoric coseismic folding along the Tsaotun segment of the Chelungpu fault near Nan-Tou, Taiwan, *J. Geophy. Res.* 112, B03S06, dori:10.1029/2006JB004493.

Suppe, J. (1981) Mechanics of mountain building and metamorphism in Taiwan, *Geol. Soc. China Mem.* 4, 67–89.

Wang, C.Y., Li, C.L., Su, F.C., Leu, M.T., Wu, M.S., Lai, S.H., Chern, C.C. (2002) Structural mapping of the 1999 Chi-chi earthquake fault, Taiwan by seismic reflection methods, *Terr. Atmo. Ocea. Sci.* 13, 211–226.

Yue, L.F., Suppe, J., Hung, J.H. (2005) Structural geology of a classic thrust belt earthquake: The 1999 Chi-Chi earthquake Taiwan (Mw = 7.6), *J. Struct. Geol.* 27, 2058–2083.
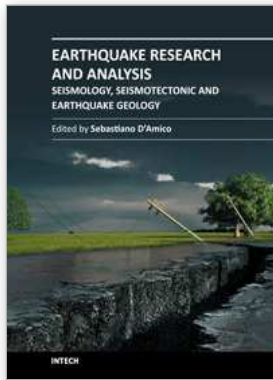
Earthquake Research and Analysis - Seismology, Seismotectonic and Earthquake Geology

Edited by Dr Sebastiano D'Amico

This book is devoted to different aspects of earthquake research. Depending on their magnitude and the placement of the hypocenter, earthquakes have the potential to be very destructive. Given that they can cause significant losses and deaths, it is really important to understand the process and the physics of this phenomenon. This book does not focus on a unique problem in earthquake processes, but spans studies on historical earthquakes and seismology in different tectonic environments, to more applied studies on earthquake geology.

How to reference

In order to correctly reference this scholarly work, feel free to copy and paste the following:

Wen-Shan Chen, Nobuhisa Matsuta and Chih-Cheng Yang (2012). Characteristics of Coseismic Thrust-Related Folding from Paleoseismic Investigation Responsible for the 1999 Chi-Chi Earthquake of Central Taiwan, Earthquake Research and Analysis - Seismology, Seismotectonic and Earthquake Geology, Dr Sebastiano D'Amico (Ed.), ISBN: 978-953-307-991-2, InTech, Available from: http://www.intechopen.com/books/earthquake-research-and-analysis-seismology-seismotectonic-and-earthquake-geology/characteristics-of-coseismic-thrust-related-folding-from-paleoseismic-investigation-responsible-for-

INTECH
open science | open minds